

# The directing role of 1,4-diazabicyclo[2,2,2]octane (DABCO)-phosphate unit in synthesis of zincophosphate faujasite (ZnPO-X)<sup>☆</sup>

Ramsharan Singh<sup>1</sup>, John Doolittle Jr., Prabir K. Dutta<sup>\*</sup>

*Department of Chemistry, The Ohio State University, 120 W. 18th Ave, Columbus, OH 43210, USA*

Received 8 January 2004; received in revised form 17 March 2004; accepted 17 March 2004

Available online 7 May 2004

## Abstract

This paper reports on the structure directing behavior of 1,4-diazabicyclo[2,2,2]octane (DABCO) in the synthesis of a faujasite-like zincophosphate framework (ZnPO-X). The nucleation of ZnPO-X occurs rapidly, within a minute of mixing of the reactants. The hypothesis we examine here is that the presence of DABCO–phosphate units in the synthesis medium accelerates the nucleation of ZnPO-X. Circumstantial evidence in support of this hypothesis was obtained from analysis of the solids formed from a combinatorial mixture of the reactants DABCO, phosphoric acid, zinc nitrate and sodium hydroxide. The synthesis systems that had the DABCO and the phosphate in the same solution tended to form ZnPO-X at a faster rate. From compositions similar to that used in synthesis of ZnPO-X, we were able to synthesize a DABCO–phosphate salt, whose structure was determined by single crystal X-ray diffraction study. Grinding a solid mixture of reactants that included the DABCO–phosphate salt led to faster formation of ZnPO-X as compared to using solid DABCO and H<sub>3</sub>PO<sub>4</sub>, providing further support for the hypothesis.

© 2004 Elsevier Inc. All rights reserved.

*Keywords:* Templating; Solid state synthesis; Zeolites; Mechanism of crystallization; Nucleation

## 1. Introduction

Microporous solids are technologically important because of their applications in petroleum, chemical and consumer industries. These materials include a large group of solids of varying chemical composition as well as porosity. The framework structure is made up of interconnecting T–O–T' bonds where T and T' can be Si, Al, P, As, Ga, Fe, Co, Zn, B and host of other elements [1,2]. The T elements are typically bonded to four oxygen atoms in a tetrahedral geometry. The best known of these materials are aluminosilicate zeolites, and synthesis of novel frameworks has the potential to lead to new technologies. However, crystal growth of these materials is a complicated process [2]. Typical syntheses

of these materials are done via hydrothermal methods, and involve rapid formation of an insoluble gel-like material, that goes through a complex sequence of depolymerization and polymerization reactions to form nuclei that grow into crystals. Various spectroscopic studies, including Raman, NMR, small angle X-ray and neutron scattering, of starting materials, intermediates and products have been carried out to study the mechanism of zeolite nucleation and crystal growth [3–7]. How microporosity is generated during such crystal growth processes is not yet clear. It has been proposed that in the presence of organic molecules, the organic–inorganic–water interactions are modified by electrostatic and hydrophobic forces to generate cavities, around which the inorganic structure links itself [7]. With enough knowledge at both the molecular and macroscopic level, synthesis by design will become possible. Towards this effort, we have investigated novel routes of microporous material crystallization. In particular, a method using reverse micelles as the source of reactants has been successfully employed in our laboratories for synthesis of microporous zincophosphates

<sup>☆</sup> Supplementary data associated with this article can be found, in the online version, at [doi:10.1016/j.micromeso.2004.03.025](https://doi.org/10.1016/j.micromeso.2004.03.025).

<sup>\*</sup> Corresponding author. Tel.: +1-6142924532; fax: +1-6146885402. E-mail address: [dutta@chemistry.ohio-state.edu](mailto:dutta@chemistry.ohio-state.edu) (P.K. Dutta).

<sup>1</sup> Present address: NeoPharm., Inc., 1850 Lakeside Drive, Waukegan, IL 60085, USA.

(ZnPO) [8–10]. Dissolution studies of ZnPO's have also provided information on the detaching/dissolving units [11].

During the past decade, zincophosphates with both condensed and open framework structure of various topologies have been reported [12–18]. The importance of amine-phosphates as intermediate species in the synthesis of zinc and other metal phosphate structures has been recognized [17,18]. In this paper, we focus on understanding the structure directing property of 1,4-diazabicyclo[2,2,2]octane (DABCO) molecule in the crystallization of ZnPO-X. By systematic variation of the order of mixing reactants for the crystallization of ZnPO-X, it was found that DABCO and phosphate ions in the same reactant solution promoted crystallization of ZnPO-X. This motivated us to isolate DABCO-phosphate crystals from a typical reactant composition and determine its crystal structure. Previous studies have reported formation of DABCO-phosphate crystals, with the DABCO molecule being doubly protonated with neutralizing  $\text{HPO}_4^{2-}$  groups [17]. Under our synthesis conditions, a singly protonated DABCO molecule with  $\text{H}_2\text{PO}_4^-$  crystal was isolated. We also report that upon mixing the DABCO-phosphate salt with other solid reactants promotes the formation of ZnPO-X. This result broadens the type of zincophosphates that can be synthesized by mixing reactants in the solid state, the only previous example being sodalite, a small pore framework [19].

## 2. Experimental

### 2.1. Materials

Zinc nitrate hexahydrate ( $\text{Zn}(\text{NO}_3)_2 \cdot 6\text{H}_2\text{O}$ ) (Aldrich, 98%), phosphoric acid ( $\text{H}_3\text{PO}_4$ ) (AR Grade, Mallinckrodt, 85%),  $\text{H}_3\text{PO}_4$  (Aldrich, 98%), 1,4-diazabicyclo[2,2,2]octane (DABCO) (Aldrich, 98%), sodium hydroxide pellets (NaOH) (98.8%, Baker Analyzed), and  $\alpha$ -alumina (99.9%, Alfa AESAR) were used as received.

### 2.2. Synthesis of ZnPO-X

Synthesis reactions of ZnPO-X were carried out following a reported literature procedure [16]. In a typical experiment, 6.5345 g (58.25 mmol) of DABCO, 0.4300 g (10.75 mmol) of NaOH, and 3.32 g of 85%  $\text{H}_3\text{PO}_4$  (28.80 mmol) were dissolved in 45 ml of water and cooled to 4 °C. To this solution was added a pre-cooled solution of 5.95 g (20.00 mmol) of  $\text{Zn}(\text{NO}_3)_2 \cdot 6\text{H}_2\text{O}$  in 5 ml of water which immediately forms a gel and was maintained at 4 °C. The crystallization process was stopped at specific times, the solids recovered and powder patterns were recorded. The relative amount of ZnPO-X was determined using  $\alpha$ -alumina as an internal

standard. In a typical method, 0.050 g of  $\alpha$ -alumina and 0.250 g of a ZnPO-X sample were mixed together in a small glass vial. The vial was capped and shaken with a Vortex Genie-2 for 5 min to ensure homogeneous mixture and then the XRD pattern was collected.

### 2.3. Synthesis of DABCO-phosphate

The preparation of DABCO-phosphate crystals was carried out by dissolving 11.218 g (100 mmol) of DABCO and 8.0 g of 85%  $\text{H}_3\text{PO}_4$  (69.38 mmol of  $\text{H}_3\text{PO}_4$ ) in 45 ml of water, with DABCO, phosphate and water at a molar ratio of 3:2.1:75. Reaction mixture became hot due to exothermic reaction. Upon cooling to room temperature, ethanol was added with vigorous stirring to induce crystallization and kept in a refrigerator overnight. The yield was 98% based on DABCO used. To grow single crystals, microcrystalline DABCO-phosphate material was dissolved in a minimum amount of water and placed in a test tube. This solution was layered with an excess of ethanol and kept aside at room temperature (25 °C). Within 3 days, single crystals of diffraction quality were observed at the interface of water solution and ethanol.

### 2.4. Crystal structure determination of DABCO-phosphate

The data was collected from a colorless rectangular chunk-like single crystal. Examination of the diffraction pattern on a Nonius Kappa CCD diffractometer indicated a triclinic crystal system. Data collection was done at 200 K using an Oxford Cryosystems Cryostream Cooler. The data collection strategy was set up to measure a hemisphere of reciprocal space with a redundancy factor of 3.8, which means that 90% of the reflections were measured at least 3.8 times. A combination of phi and omega scans with a frame width of 1.0° was used. Data integration was done with Denzo, and scaling and merging of the data was done with Scalepack [20]. Merging the data and averaging the symmetry equivalent reflections resulted in an  $R_{\text{int}}$  value of 0.028. The teXsan [21] package indicated the space group to be  $P\bar{1}$  based on the intensity statistics. Relevant details of the single crystal structure determination of the DABCO-phosphate are presented in the Supplementary Information Section.

The structure was solved by direct methods in SHELXS-86 [22]. The asymmetric unit consists of  $\text{H}_2\text{PO}_4^-$ , a singly protonated DABCO molecule, and a water molecule. Full-matrix least-squares refinements based on  $F^2$  were performed in SHELXL-93 [23]. The hydrogen atoms bonded to carbon atoms were included in the model at calculated positions using a riding model with  $U(H) = 1.2 * U(\text{eq})$  (attached atom). All of the other hydrogen atoms were located on a difference

electron density map and refined isotropically. The final refinement cycle was based on all 2306 intensities and 147 variables and resulted in agreement factors of  $R_1(F) = 0.034$  and  $wR_2(F^2) = 0.085$ . For the subset of data with  $I > 2\sigma(I)$ , the  $R_1(F)$  value is 0.030 for 2084 reflections. The final difference electron density map contains maximum and minimum peak heights of 0.25 and  $-0.42 \text{ e}/\text{\AA}^3$  respectively. Neutral atom scattering factors were used and include terms for anomalous dispersion.

### 2.5. Synthesis by mixing reactants in the solid state

Synthesis of ZnPO-X by grinding together solid reactants was performed in two ways:

*Reactions using  $\text{H}_3\text{PO}_4$  as a source of phosphate ions.* Solid ingredients,  $\text{Zn}(\text{NO}_3)_2 \cdot 6\text{H}_2\text{O}$ ,  $\text{H}_3\text{PO}_4$ , DABCO and NaOH were used as reactants. Reaction compositions were similar to those for normal solution synthesis, but with no added water. In a typical experiment 1.6336 g (14.56 mmol) of DABCO, 0.7199 g (7.2 mmol) of  $\text{H}_3\text{PO}_4$  (98%), 0.1075 g (2.69 mmol) of NaOH and 1.4875 g (5.00 mmol) of  $\text{Zn}(\text{NO}_3)_2 \cdot 6\text{H}_2\text{O}$  were mixed in a mortar pestle under dry  $\text{N}_2$  to start the reaction, and maintained in this state for the duration of the reaction (in a glovebag).

*Reactions using DABCO-phosphate as a source of phosphate ions.* In this experiment, DABCO-phosphate was used as the source of phosphate. To match the reaction composition to the  $\text{H}_3\text{PO}_4$ -based synthesis, additional amount of DABCO was needed. In a typical experiment 1.6427 g (7.20 mmol) of DABCO-phosphate, 0.8260 g (7.36 mmol) of DABCO, 0.1075 g (2.69 mmol) of NaOH and 1.4875 g (5.00 mmol) of  $\text{Zn}(\text{NO}_3)_2 \cdot 6\text{H}_2\text{O}$  were mixed in a mortar and pestle to start the reaction and were maintained under dry  $\text{N}_2$ .

### 2.6. Characterization

The X-ray powder patterns were determined with a Bruker D-8 X-ray diffractometer using nickel-filtered  $\text{Cu K}\alpha$  ( $\lambda = 1.5405 \text{ \AA}$ ) radiation. Elemental analysis was performed by Galbraith Laboratories, Tennessee.

## 3. Results

### 3.1. Synthesis of ZnPO-X

The kinetics of the crystallization of hydrothermal synthesis of ZnPO-X is shown in Fig. 1. For this study, a series of reactions were set up. The products were isolated at certain times and XRD patterns were recorded. The sample recovered from these experiments was pure ZnPO-X as determined by comparison with literature [12,16,24]. Using  $\alpha$ -alumina as an internal standard ( $2\theta = 37.8^\circ$ ), the increase in the amount of ZnPO-X ( $2\theta = 30.7^\circ$ ) in the product mixture was monitored (standard deviations of the XRD measurements using  $\alpha$ -alumina as standard was  $<2\%$ ). The choice of the  $2\theta = 30.7^\circ$  peak for ZnPO-X was made based on its proximity to the  $\alpha$ -alumina standard. Crystals were found within the first minute and the crystallization process was complete within the first 10–20 min.

### 3.2. Reactions using different combinations of reactants

Reactions using different combinations of reagents split into two reactants, but with overall similar composition were set up as outlined in Table 1. These

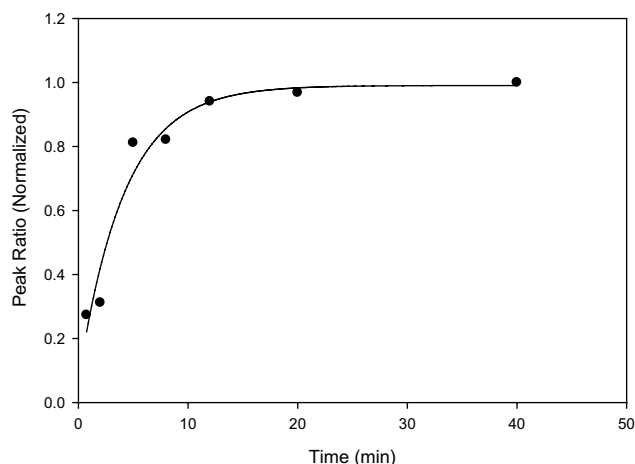


Fig. 1. Growth curve for ZnPO-X synthesis using Reaction 1 of Table 1. The y-axis is the ratio of the intensity of the ZnPO-X peak at  $2\theta = 30.7^\circ$  versus an internal standard alumina peak at  $2\theta = 37.8^\circ$ .

Table 1

Reaction sequence

Reaction	Reactant A	Reactant B	Products at 1 min
1	$\text{Zn}(\text{NO}_3)_2$	DABCO + NaOH + $\text{H}_3\text{PO}_4$	ZnPO-X + Hopeite (minor)
2	$\text{Zn}(\text{NO}_3)_2 + \text{H}_3\text{PO}_4$	DABCO + NaOH	Hopeite + ZnPO-X (minor)
3	$\text{Zn}(\text{NO}_3)_2 + \text{DABCO} + \text{H}_3\text{PO}_4$	NaOH	Hopeite
4	$\text{Zn}(\text{NO}_3)_2 + \text{DABCO} + \text{NaOH}$	$\text{H}_3\text{PO}_4$	Amorphous + Hopeite (minor) + ZnPO-X (minor)
5	$\text{Zn}(\text{NO}_3)_2 + \text{NaOH}$	DABCO + $\text{H}_3\text{PO}_4$	ZnPO-X + Hopeite (minor)
6	$\text{Zn}(\text{NO}_3)_2 + \text{DABCO}$	NaOH + $\text{H}_3\text{PO}_4$	Amorphous solid + ZnPO-X + Hopeite
7	$\text{Zn}(\text{NO}_3)_2 + \text{H}_3\text{PO}_4 + \text{NaOH}$	DABCO	ZnPO-X + Hopeite (minor)

reactants were mixed and solid products were recovered from the solutions at periodic intervals of 1 min, 30 min, 1 h and 2 h. The XRD patterns of the products indicated that all six reactions produced ZnPO-X within 30 min. Thus, in order to investigate the initial rates of formation, we have focused on the products present after the first minute of reaction and are listed in Table 1. Fig. 2 shows the XRD patterns of the reaction products recovered after 1 min from reactions 5 (Fig. 2a) and 2 (Fig. 2b). The products were not washed prior to the diffraction experiments. As exemplified by Fig. 2, the primary products of the reactions were ZnPO-X (marked as X in Fig. 2) and hopeite (marked as H,  $\text{Zn}_3(\text{PO}_4)_2 \cdot 4\text{H}_2\text{O}$ ). These assignments were based on pure compounds synthesized in the laboratory and are also consistent with literature reports [24–26]. (Hopeite is JCPDS file no. 33-1474.) It is important to note that for the weak overlapping peaks in Fig. 2, there is some ambiguity in assignment of the peaks, since there could be slight shifts in the peaks, even though all samples were conditioned similarly.

Except for Reaction 3, in all other cases, ZnPO-X emerges as the initial major product when DABCO and phosphate are in the same reactant batch. In cases such as Reaction 2, the presence of phosphoric acid and zinc ions in the same reactant mixture led to rapid precipitation of hopeite, thus impeding the association of DABCO and phosphate. However, for Reaction 7, presence of all three components, zinc ion, phosphate and hydroxide led to a clear solution (Reactant A), which upon reaction with a DABCO solution produced ZnPO-X as the major species. In this system, the DABCO was free to associate with the phosphate species upon mixing because Reactant A was a homogeneous solution.

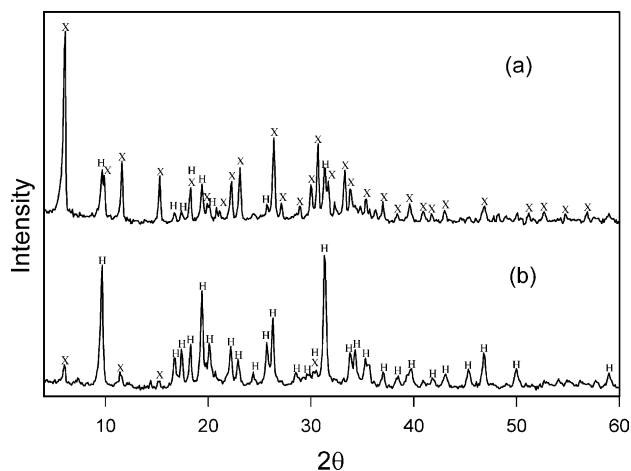


Fig. 2. Comparison of the diffraction patterns of products recovered from reactions one minute after mixing two reactants. (a) Reactant A =  $\text{Zn}(\text{NO}_3)_2 + \text{NaOH}$ , Reactant B = DABCO +  $\text{H}_3\text{PO}_4$ ; (b) Reactant A =  $\text{Zn}(\text{NO}_3)_2 + \text{H}_3\text{PO}_4$ , Reactant B = DABCO + NaOH. (X = ZnPO-X; H = Hopeite.)

### 3.3. Isolation and structure of the DABCO–phosphate salt

From a clear solution with a molar composition of DABCO: $0.7\text{H}_3\text{PO}_4$ : $25\text{H}_2\text{O}$ , crystals were produced by inducing precipitation with ethanol at ambient temperature. A composition based on the ZnPO-X system (without  $\text{Zn}^{2+}$ , DABCO: $0.5\text{H}_3\text{PO}_4$ : $43\text{H}_2\text{O}$ ) also produces a similar DABCO–phosphate salt, as verified by powder diffraction data (not shown). The ORTEP diagram of the asymmetric unit of DABCO–phosphate is given in Fig. 3a and the unit cell diagram is shown in Fig. 3b. The structure consists of a 1:1 adduct of  $\text{H}_2\text{PO}_4^-$  and singly protonated DABCO molecule with one molecule of water of hydration. The structure forms a sheet with alternating phosphate and DABCO molecules linked via the water molecule. There is extensive hydrogen bonding in the crystal structure of DABCO–phosphate. The donor–H...acceptor angles are  $>171^\circ$  indicating strong hydrogen bonding (Supplementary Information Table 1). Table 2 compares the crystal data and structure refinement parameters for the complex synthesized in this study with a similar complex but with doubly protonated DABCO and  $\text{HPO}_4^{2-}$  [17b]. Further details on the atomic coordinates for the DABCO–

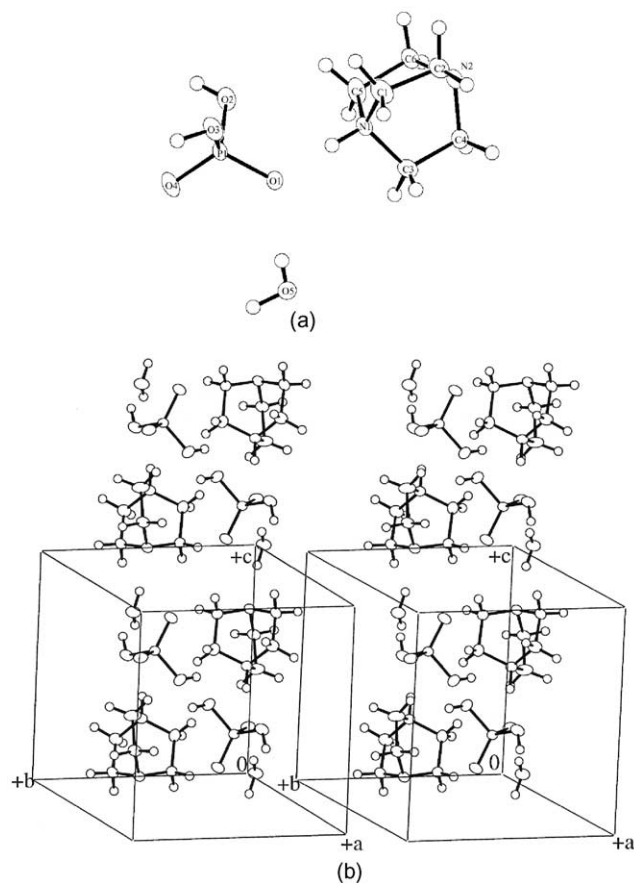


Fig. 3. (a) Asymmetric unit of the DABCO–phosphate complex. (b) Unit cell diagram of the DABCO–phosphate complex.

Table 2  
Crystal data and structure refinement parameters for DABCO-phosphate

Empirical formula	C <sub>6</sub> H <sub>17</sub> N <sub>2</sub> O <sub>5</sub> P	C <sub>6</sub> H <sub>17</sub> N <sub>2</sub> O <sub>5</sub> P
Crystal system	Triclinic	Triclinic
Space group	$P\bar{1}$	$P\bar{1}$
Formula mass	228.19	228.19
Crystal size (mm <sup>3</sup> )	0.12 × 0.19 × 0.27	0.12 × 0.12 × 0.24
<i>a</i> (Å)	6.8783(1)	6.906(2)
<i>b</i> (Å)	8.9319(1)	9.018(4)
<i>c</i> (Å)	9.2555(2)	9.271(2)
$\alpha$ (deg)	92.070(1)	92.21(3)
$\beta$ (deg)	104.611(1)	104.51(2)
$\gamma$ (deg)	111.814(1)	111.76(2)
<i>V</i> (Å <sup>3</sup> )	505.470(14)	513.5(3)
Calculated density (mg/m <sup>3</sup> )	1.499	1.476
<i>Z</i>	2	2
$\lambda$ (Mo K $\alpha$ ) (Å)	0.71073	0.71073
Absorption coefficient, $\mu$ (mm <sup>-1</sup> )	0.274	0.27
$\theta$ range (deg)	2.30–27.47	2.46–23.27
Reflections collected	15745	2176
Index ranges	$-8 \leq h \leq 8, -11 \leq k \leq 11, -12 \leq l \leq 11$	$-7 \leq h \leq 7, -9 \leq k \leq 10, -10 \leq l \leq 10$
Independent reflections	2306	1448
Data/restraints/no. of parameters	2306/0/147	1397/0/136
<i>R</i> indices ( $I > 2\sigma(I)$ )	$R_1 = 0.0302$	$R_1 = 0.04$
$wR_2$ ( $I > 2\sigma(I)$ )	0.0818	0.10
$R_1$ (all data)	0.0342	–
$wR_2$ (all data)	0.0845	–
GOF	1.051	1.107
Refinement method	Full-matrix least-squares on $F^2$	–
Largest diff. peak and hole	0.245 and $-0.420$ e/Å <sup>3</sup>	–
<i>F</i> (000)	244	–
Ref.	This work	Ref. [17b]

phosphate complex as well as the bond lengths, angles and hydrogen bond lengths and angles are provided in the Supplementary Information Section.

The DABCO-phosphate polycrystalline powder isolated by ethanol-induced precipitation gave the following elemental analysis: P-14.05%, C-33.05%, H-7.22%, N-12.86%, and matched best with the formula N(CH<sub>2</sub>CH<sub>2</sub>)<sub>3</sub>NH<sup>+</sup>H<sub>2</sub>PO<sub>4</sub><sup>-</sup>·0.5H<sub>2</sub>O, whereas the formula calculated from the single crystal data suggests a structure with one molecule of water of hydration.

### 3.4. Synthesis of ZnPO-X by mixing reactants in the solid state

Two sets of syntheses were carried out by mixing solid reactants using either H<sub>3</sub>PO<sub>4</sub> or DABCO-phosphate salt as the source of phosphate ions, the other reagents being crushed NaOH and Zn(NO<sub>3</sub>)<sub>2</sub>·6H<sub>2</sub>O. Care was taken to ensure that the overall composition in both sets of reactions was identical and the reaction was done under dry N<sub>2</sub>. After the initial grinding, the reaction was allowed to proceed undisturbed and samples were collected over a 50 h time frame and the diffraction patterns measured (under similar conditions). Fig. 4a and b compare the XRD pattern of samples recovered from DABCO-phosphate and H<sub>3</sub>PO<sub>4</sub>, respectively after

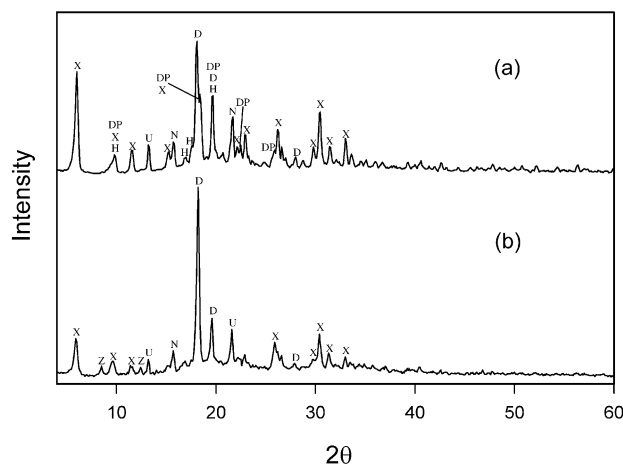


Fig. 4. Diffraction patterns from solid-state synthesis after 50 min of reaction (unwashed). (a) DABCO-phosphate complex as reagent; (b) DABCO and H<sub>3</sub>PO<sub>4</sub> are separate reagents. (X = ZnPO-X; H = Hopeite; D = DABCO; DP = DABCO-phosphate; Z = ZnHPO<sub>4</sub>; N = Zn(NO<sub>3</sub>)<sub>2</sub>·6H<sub>2</sub>O; U = undetermined.)

50 min of reaction (samples were not washed, data collected under identical conditions). The material prepared with the DABCO-phosphate salt exhibits stronger peaks of ZnPO-X. Along with ZnPO-X (X) and hopeite (H), unreacted DABCO (D; JCPDS file no.

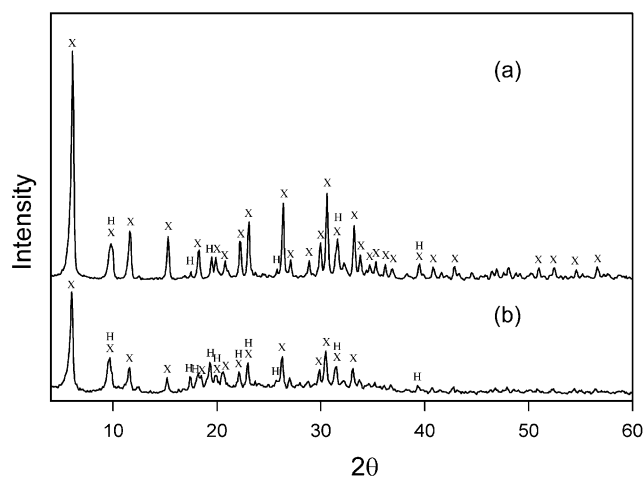


Fig. 5. Diffraction from solid-state synthesis after 50 h of reaction (products washed with ethanol). (a) DABCO–phosphate complex as reagent; (b) DABCO and  $\text{H}_3\text{PO}_4$  are separate reagents. (X = ZnPO-X; H = Hopeite.)

21-1617) [26], DABCO–phosphate (DP, assignment made based on this study) and  $\text{Zn}(\text{NO}_3)_2 \cdot 6\text{H}_2\text{O}$  (N, based on this study) were also observed. In the case of the reaction with  $\text{H}_3\text{PO}_4$ , peaks at  $8^\circ$  and  $12^\circ$  are typical of  $\text{ZnHPO}_4$  (JCPDS, 37-0315) [26]. Fig. 5 compares the XRD pattern after 50 h of reaction (samples washed with ethanol and data collected under identical conditions). Ethanol was used as solvent to avoid any transformation of reactants via contact with water. Crystals obtained from the reactant using DABCO–phosphate salt (Fig. 5a) were purer with relatively lower hopeite contribution.

#### 4. Discussion

The focus of this discussion is on the role of DABCO in crystallization of ZnPO-X. The induction time for the hydrothermal synthesis of ZnPO-X in the presence of DABCO is very short, occurring in less than a minute. Indeed, the motivation for the present study was to explore how DABCO accelerates ZnPO-X crystallization under such mild thermal conditions. Single crystal structure of novel zincophosphate open frameworks using DABCO as a structure directing agent have also been reported, showing the generality of this molecule as a structure directing agent [27–29].

There were two reasons to explore if a DABCO–phosphate unit was acting as an intermediary in the crystallization process of ZnPO-X. First, a DABCO–phosphate unit has been crystallized, suggesting its stability [17]. Moreover, it has also been reported that addition of the DABCO–phosphate complex to  $\text{Zn}^{2+}$  did produce ZnPO phases similar to when DABCO and  $\text{H}_3\text{PO}_4$  were added independently [18]. Also, it was found that DABCO–phosphate will react with  $\text{Zn}^{2+}$  to

produce frameworks under considerably milder conditions [18,27]. Second, as we show in Table 1, ZnPO-X is nucleated more rapidly when DABCO and the phosphate are in the same reactant solution at the earliest stage of the synthesis. This suggests that association of DABCO and phosphate can promote ZnPO-X nucleation.

The DABCO–phosphate unit that crystallized from the reaction composition DABCO:0.7 $\text{H}_3\text{PO}_4$ :25 $\text{H}_2\text{O}$  in this study is slightly different from the complex reported earlier [17]. The crystallization was induced by addition of excess ethanol to a clear solution at ambient temperature and the crystals consisted of a singly protonated DABCO molecule with  $\text{H}_2\text{PO}_4^-$  as the neutralizing anion. In the previous study [17], DABCO–phosphate was crystallized from a more concentrated solution (DABCO: 1–2 $\text{H}_3\text{PO}_4$ :5 $\text{H}_2\text{O}$ ) and contained a doubly protonated DABCO with  $\text{HPO}_4^{2-}$  as the neutralizing group, and proceeded through an amorphous gel and needed to be heated to  $110^\circ\text{C}$  for 6 h to produce plate-like crystals. However, both units crystallize in triclinic space group  $P\bar{1}$  and the unit cell dimensions and volumes are comparable, with the monoprotonated DABCO species resulting in a more compact unit cell. The detailed crystal data for both systems are compared in Table 2.

Evidence about the role of the DABCO–phosphate unit in directing the formation of ZnPO-X is also provided by the synthesis involving the solid-state reactants, where the presence of the salt led to an acceleration of the formation of ZnPO-X as well as higher purity. Even though no water was added to the solid-state synthesis reactions and they were kept under ambient conditions, the mixtures became moist due to the hydration water present in the reactants. A similar effect was reported for the solid-state synthesis of zincophosphate sodalite [19]. In the reaction system using DABCO and anhydrous  $\text{H}_3\text{PO}_4$ , there is the possibility of association of these two species prior to ZnPO-X crystallization, considering the moist environment (the formation of  $\text{ZnHPO}_4$  as an intermediate supports this idea). However, because of the necessity of association, the rate of crystallization is slower with the individual reactants as compared to the reaction using the DABCO–phosphate salt.

For cobaltophosphate synthesis, it was proposed that the DABCO–phosphate complex may orient the  $\text{H}_2\text{O}$  molecules in a specific geometry [17]. These  $\text{H}_2\text{O}$  molecules are then replaced by  $\text{Co}^{2+}$  on the path to bonding with phosphate to form the framework. The exact role by which the DABCO–phosphate complex directs the formation of ZnPO-X is unclear, especially in a typical hydrothermal synthesis. It is doubtful that the amine-phosphate indeed survives as a structural unit during the reaction, as amine-phosphates are highly water soluble. The solid-state experiments reported here indicate that presence of preexisting DABCO–phosphate structural

units do promote the formation of ZnPO-X, and even loosely arranged DABCO-phosphate units in solution may be able to promote the nucleation of ZnPO-X. The other possibility is that the synthesis is mediated by zinc phosphate primary building units [30]. Attempts at isolating such units from the ZnPO-X synthesis medium were unsuccessful.

Finally, the demonstration of the synthesis of ZnPO-X open framework structure by mixing solid reactants opens up a pathway to entrap large molecules in the supercages, as has been recently reported for sulfur and CdS entrapment in sodalite [19].

## 5. Conclusions

The hypothesis tested in this paper is that DABCO and phosphate reactants can form DABCO-phosphate units that accelerate the nucleation of ZnPO-X. It was found that DABCO and phosphate in the same reactant solution nucleated ZnPO-X faster as compared to reactions where DABCO and phosphate were in different solutions. A DABCO-phosphate salt was crystallized from reaction mixtures typical for the formation of ZnPO-X (in the absence of Zn<sup>2+</sup>) and its structure determined by diffraction. The rate of synthesis of ZnPO-X by mixing solid reactants was faster with DABCO-phosphate salt than when phosphoric acid and DABCO were separate, further suggesting the acceleration of ZnPO-X nucleation by DABCO-phosphate structural units.

## Acknowledgements

We acknowledge funding from NASA for this research. We thank Dr. J. Gallucci for single crystal X-ray structure determination of the DABCO-phosphate complex. Supplementary information detailing the crystal structure of DABCO-phosphate complex is also provided.

## References

- [1] R. Szożak, *Handbook of Molecular Sieves*, Van Nostrand, New York, 1992.
- [2] S.M. Auerbach, K.A. Carrado, P.K. Dutta (Eds.), *Handbook of Zeolite Science and Technology*, Marcel-Dekker, 2003.
- [3] P.K. Dutta, *Journal of Inclusion Phenomena Mol. Recognit. Chem.* 21 (1995) 215.
- [4] G. Engelhardt, H. van Koningsveld, *Zeolites* 10 (1990) 650.
- [5] C.E.A. Kirschock, R. Ravishankar, P.A. Jacobs, J.A. Martens, *Journal of Physical Chemistry B* 103 (1999) 11021.
- [6] D.D. Kragten, J.M. Fedeyko, K.R. Sawant, J.D. Rimer, D.G. Vlachos, R.F. Lobo, *Journal of Physical Chemistry B* 197 (2003) 10006.
- [7] D.P. Serrano, S. van Grieken, *Journal of Materials Chemistry* 11 (2001) 2391.
- [8] R. Singh, J. Doolittle Jr., M.A. George, P.K. Dutta, *Langmuir* 18 (2002) 8193.
- [9] R. Singh, P.K. Dutta, *Langmuir* 16 (2000) 4148.
- [10] R. Singh, M. Castagnola, P.K. Dutta, in: J. Texter (Ed.), *Reactions and Synthesis in Surfactant Systems*, Marcel-Dekker, New York, 2001, pp. 737–760.
- [11] R. Singh, J. Doolittle Jr., P.K. Dutta, *Journal of Physical Chemistry B* 106 (2002) 2146.
- [12] T.E. Gier, G.D. Stucky, *Nature* 349 (1991) 508.
- [13] T.M. Nenoff, W.T.A. Harrison, T.E. Gier, G.D. Stucky, *Journal of the American Chemical Society* 113 (1991) 378.
- [14] S. Neeraj, M.L. Noy, C.N.R. Rao, A.K. Cheetham, *Solid State Sciences* 4 (2002) 1231.
- [15] A.R. Cowley, R.H. Jones, S.J. Teat, A.M. Chippindale, *Microporous and Mesoporous Materials* 51 (2002) 51.
- [16] S. Feng, T. Bein, *Nature* 368 (1994) 834.
- [17] (a) C.N.R. Rao, S. Natarajan, S. Neeraj, *Journal of Solid State Chemistry* 152 (2000) 302;  
(b) S. Natarajan, S. Neeraj, C.N.R. Rao, *Solid State Sciences* 2 (2000) 87.
- [18] S. Neeraj, S. Natarajan, C.N.R. Rao, *Angewandte Chemie International Edition* 38 (1999) 3480.
- [19] S. Kowalak, A. Jankowska, E. Baran, *Chemical Communications* 6 (2001) 575.
- [20] DENXO: Z. Otwinowski, W. Minor, *Methods in Enzymology*, in: C.W. Carter Jr., R.M. Sweet (Eds.), *Macromolecular Crystallography, Part A*, vol. 276, Academic Press, 1997, pp. 307–326.
- [21] teXsan: *Crystal Structure Analysis Package*, Ver. 1.7-2, Molecular Structure Corporation, The Woodlands, TX, 1995.
- [22] SHELXS-86: G.M. Sheldrick, *Acta Crystallographica A* 46 (1990) 467.
- [23] SHELXL-93: G.M. Sheldrick, *Universitat Gottingen, Germany*, 1993.
- [24] M.M.J. Tracy, J.B. Higgins, *Collection of Simulated ORD Powder Patterns for Zeolites*, Elsevier Science, Amsterdam, 2001.
- [25] G. Lusvardi, L. Menabue, M. Saladini, *Journal of Materials Science: Materials in Medicine* 13 (2002) 91.
- [26] XRD Pattern Processing software (JADES) titled MDI Jade 5.0.18, *Materials Data, Inc.*, Livermore, California. Available from <www.materialsdata.com>.
- [27] W.T.A. Harrison, T.E. Martin, T.E. Gier, G.D. Stucky, *Journal of Materials Chemistry* 2 (1992) 175.
- [28] J. Li, Y. Ke, Y. Zhang, G. He, Z. Jiang, M. Nishiura, T. Imamoto, *Journal of the American Chemical Society* 122 (2000) 6110.
- [29] G. Schafer, W. Carrillo-Caberra, S. Leoni, H. Borrmann, R.Z. Kniep, *Anorg. llg. Chem.* 628 (2002) 67.
- [30] S. Neeraj, S. Natarajan, C.N. Rao, *Journal of Solid State Chemistry* 150 (2000) 417.